

1 **On the search for the source of the 1865-66 Nicaraguan earthquakes:**

2 **paleoseismic data from the Cofradía fault, Managua**

3 **graben(Nicaragua)**

4 P. Santanach¹, P. Ruano², M. Ortuño¹, C. Rubí³ and E. Masana¹

5 1) Dpt. de Geodinàmica i Geofísica, Grup RISKINAT, Universitat de Barcelona

6 2) Dpto de Geodinàmica, Fac. de Ciencias., Universidad de Granada

7 3) CIGEO, Universidad Nacional de Nicaragua, Managua

8 Address of corresponding author: maria.ortuno@ub.edu

9
10 Several catastrophic earthquakes struck Managua during the last few centuries. Among
11 the seismogenic fault systems causing them, only two of them have been previously
12 studied through a paleoseismological approach. In this paper, we present new data
13 supporting that the Cofradia fault is a seismogenic fault and the most probable source of
14 the 1865-1866 Nicaraguan earthquakes (Intensity = X). The data were collected at three
15 paleoseismological sites, two of them located on the main trace; La Vaqueria (central-
16 northern part) and El Cocal (central part); and the other one, Piedra Menuda, on an
17 antithetic strand of the southern fault segment. Coseismic evidence consists of
18 liquefaction features, offset layers and colluvial wedges dated with radiocarbon ages and
19 relative cultural ages attributed to pottery fragments. The minimum event displacement
20 observed at the central site, 1 m, and the total length of the mapped geomorphological
21 trace, 39 km, are consistent with maximum expected magnitudes around 7. A minimum
22 slip rate between 1.1 – 1.3 mm/yr is obtained from the new data, reinforcing the previous
23 estimates. The paleoseismic chronology points towards the occurrence of at least three
24 seismic events since 1650 yr BP, the last one occurring after 1281 cal yr BP and shortly
25 Before Present. Accordingly, the damaging earthquakes of 1865-1866 causing surface
26 alterations in the Tipitapa river could have been produced by the last paleoseismic event
27 on the Cofradia fault. This match leads to an estimated recurrence period between 624 yr
28 and 783 yr for the maximum expected events on this fault.

29

30 Online Material: High-resolution photomosaics of trench exposures (Figures S1, S2, and
31 S3)

32

33 **Introduction**

34 Shallow earthquakes affect repeatedly Managua Metropolitan area, Nicaragua,
35 which lodges more than 2,000,000 people. Managua is built on a graben, whose faults are
36 responsible for the localeismicity. Two destructive earthquakes, which ruptured the
37 surface, occurred within the graben during the 20th century: On March 31, 1931 an
38 earthquake of magnitude mb5.6 (Leeds, 1974) destroyed the city of Managua with about
39 1,000 fatalities of a population of about 40,000 (Durham, 1931; Sultan, 1931), and on
40 December 23, 1972 a M_s 6.2 earthquake again destroyed the city (ca. 500,000 inhabitants)
41 killing about 11,000 people and injuring more than 20,000 (Brown et al., 1973). In the
42 19th century, from December 1865 to February 1866, strong earthquakes struck western
43 Nicaragua affecting León, Managua and Granada. It was reported that the Tipitapa River,
44 which drains the Managua Lake into the Nicaragua Lake to the East (Fig. 1), “suffered
45 remarkable topographic changes” during these earthquakes (Montessus de Ballore, 1888).
46 On the basis of Montessus description, taken from Grases(1974),Peraldo and Montero
47 (1999)located the epicentral area of these earthquakes on the Cofradía fault, which bounds
48 the Managua graben to the East and crosses the Tipitapa River at Tipitapa. The Cofradia
49 fault is 39 km long and therefore capable ofgenerate hazardous earthquakes affecting
50 Managua.

51

52 Accepting the hypothesis of Peraldo and Montero, we carried out
53 paleoseismological research on the Cofradia fault with the aim to obtain seismological
54 parameters (Length, slip rate, recurrence) of this fault, as a contribution to the
55 understanding of the seismological hazard of Managua Metropolitan area.

56

57

58 **The Managua graben and the Cofradía fault**

59 The Central American Volcanic Chain, is developed in relation to the subduction
60 of the Cocos plate below the Caribbean plate. Some of its volcanoes are located along the
61 Nicaraguan Depression (back arc basin; [De Mets et al., 1994](#); [Alvarado et al., 2011](#)),
62 which extends from El Salvador to Costa Rica and separates the Tertiary igneous rocks
63 of the interior highlands from the marine sedimentary rocks of the Pacific coastal hills
64 (**Fig. 1a**). It began to form at the Early Neogene ([Funk et al., 2009](#)), and it is filled up by a
65 large volume of Quaternary volcanoclastic deposits. Within the Nicaraguan depression,
66 the N-S oriented Managua graben was formed on a relay zone. It has a length of ca. 40 km
67 and a width of approximately 20 km.

68 Since the 1972 M 6.2 earthquake, a number of different tectonic interpretations of
69 the Managua graben and its relation to the Nicaraguan depression, the volcanic chain and
70 the subduction zone have been published and relate it to transform faulting and bookshelf
71 faulting models (i.e.: [Ward et al., 1974](#); [Dewey and Algermissen, 1974](#); [Ferrez-Weinberg,](#)
72 [1992](#); [Frischbutter, 2002](#); [Cowan et al., 2002](#); [La Femina et al., 2002](#); [Girard and van Wyk](#)
73 [de Vries, 2005](#); [Funk et al., 2009](#)).

74 Submeridional faults bound the Managua graben, the Nejapa-
75 Miraflores alignment to the west and the Cofradía fault to the east (**Fig. 1b**). In its interior,
76 NE-SW left lateral strike-slip faults stand out, as the Estadio fault responsible for the 1931
77 earthquake and the Tiscapa fault and the related faults which caused the 1972 earthquake
78 ([Brown et al., 1973](#); [Ward et al., 1974](#)).

79 Paleoseismological data from the Aeropuerto fault (**Figs. 1b and 1c**) in the
80 vicinity of Managua has been published by [Cowan et al., \(2002\)](#). This fault is parallel and

81 antithetic to the Cofradía fault, and both faults bound the deeper, eastern portion of the
82 Managua graben (Martínez and Noguera, 1992). The most recent large earthquake on the
83 Aeropuerto fault occurred during the interval 300-140yr BP (Cowan et al., 2002). It could
84 correspond to one of the three largest earthquakes reported in the Managua/Granada
85 region during this time interval. These are the earthquakes of 1663, 1764, and 1772
86 (Leeds, 1974), coinciding with volcanic unrest and eruptions from volcanoes in the
87 region. An earlier earthquake on this fault occurred prior to 560 yr BP and possibly around
88 2000 yr BP. Cowan et al. (2002) have estimated a vertical slip rate of 0.3 to 0.9 mm/yr
89 along the Aeropuerto fault.

90

91 The Cofradia fault trends N-NNE, dips steeply to the west and runs from the
92 Masaya volcano, to the North limiting the graben to the east (Fig. 1b and c). The fault
93 consists of a number en echelon segments that show W-facing scarps reaching heights up
94 to 15 m and minor antithetic scarps (Fig. 1c). These segments offset several drainage
95 networks that evidence young fault activity with mainly dip slip, but also some left lateral
96 motion. Dames and Moore-Lansa (1978) have demonstrated by means of
97 trenching through some of these scarps in the vicinity of the Tipitapa River (Fig. 1c) that
98 scarps correspond to the relief created by Holocene activity of different strands of the
99 Cofradía fault. They have also documented 5000±1000yr old lake deposits about six
100 meters above the modern lake shoreline. On this basis, Cowan et al. (2000) have suggested
101 a slip rate of 1.2 mm/yr for the Cofradía fault.

102

103 **Method**

104 The approach used was a standard paleoseismological study, involving: 1) A
105 geomorphological survey by means of 1:33,000 scale aerial photographs of the Cofradia

106 fault and surroundings. 2) A field survey along the fault to study in more detail some
107 sectors to select the most suitable sites for trenching. 3) Topographic leveling of
108 topographical profiles and maps (0.5 m contour levels) of the selected sites. 4) Digging
109 four trenches, logging its walls and collecting samples for dating. 5) Interpreting the
110 obtained data in terms of paleoseismic events and parameters.

111

112 To constrain the age of paleoseismic events, a number of samples of different
113 materials were collected from different stratigraphical units: coals and woods, a deer leg
114 bone fragment, lacustrine bivalve mollusc shells, bulk soil samples and pottery fragments.
115 Ages derived from ^{14}C dating of bivalve mollusc shells and charcoal fragments were
116 obtained at the Accelerator Mass Spectrometry *NOSAMS* laboratory
117 (Universitat Autònoma de Barcelona). All ^{14}C laboratory ages were calibrated and given
118 as 2σ interval (95% of confidence) and adjusted to the nearest decade, according to the
119 Calib7.1 software (Stuiver and Reimer, 1993) and the INTCAL13 curves (Reimer et al.,
120 2013). Pottery fragments have been examined and attributed to particular prehispanic
121 cultures by E. Espinosa (Director of the Museo Nacional de Nicaragua). The proposed
122 time spans for the different cultures are those used by García Vázquez (1996). All ages
123 are in yr BP or cal yr BP (^{14}C dates) for better correlation.

124

125 **Trenching on the Cofradía fault**

126

127 Looking for recent seismic events, we dug trenches in three sites on the southern
128 part of the Cofradía fault, named, from N to S, La Vaquería, El Cocal y La
129 Piedra Menuda (Fig. 1c). The El Cocal trench yielded most of the relevant paleoseismic
130 data, part of which has been presented in Ruano et al. (2008).

131

132 *El Cocal trench site*

133 The Cofradía fault scarp is characterized by linear segments between Masaya
134 volcano and Managua Lake. It becomes sinuous at the El Cocal site, at the shore of the
135 Managua Lake, where it is eroded and slightly retreated and the fault trace is covered by
136 lacustrine terrace deposits. We excavated a 28 m long and 2.5 m deep trench,
137 perpendicular to the general trend of the fault scarp, in front of the eroded scarp (Fig. 1c).
138 The fault was located 17 m to the west of the present geomorphological scarp.

139 Two stratigraphic groups deposited under different sedimentary environments can
140 be identified (Fig. 2a, supplementary Figure S1). From base to top, Group 1 presents
141 2.2 m minimum thickness and it is made of three units of lacustrine sediments (*w-*
142 *y*). Within them, a sandy layer (*x*) can be used as a guide level inside this
143 group. Liquefaction structures affect layer *x* and layers just beneath it. At the toe of the
144 morphological scarp, the described units are overlain by a wedge of conglomerate with
145 clayish matrix and alternating levels of sands and pebbles of possible fluvial origin (*z*).

146

147 Group 2 (units *e-a*) unconformably lies on top of the first group. Unit (*e*) with
148 triangular shape consists of a clast-supported breccia presenting non-stratified structure,
149 coarse sand to gravel matrix and heterometric clasts from the *w-y* sequence, which
150 reach up to 50 cm in diameter. On top of it, two units are found: unit (*d*) consists of green
151 clay, rich in sand with dispersed sharp pumice clasts overlain by a micro-conglomerate (unit
152 *c*) showing an erosive base and liquefaction structures, with abundant coal pieces.

153

154 Unconformably over the units of both groups, top unit (*a*) is a massive matrix-
155 supported conglomerate containing 2-10 cm clasts of pumice embedded in volcanic ash

156 and compacted clay that turn into a sandy matrix breccia eastwards (unit *b*). The present
157 day soil (unit *s*) caps the aforementioned units.

158 In the eastern part of the trench, the units of the Group 1 are horizontal and become
159 inclined towards the W in the central part, describing a flexure. The flexure zone is
160 affected by a set of high angle normal faults, which probably correspond to an upwards
161 splay of the deeper main Cofradía fault. The units of Group 2 unconformably lay on the
162 described flexure, and are partially affected by these normal faults.

163

164 *La Vaquería trench site*

165 Two trenches 17 m long were dug on a 3 m high westward facing scarp partially
166 covered by alluvial fan deposits (**Fig. 1c, Fig. 2b, supplementary Figure S2**). The up-
167 thrown block consists of volcanic air-fall deposits (units 1 to 4), and the downthrown
168 block consists of alluvial fan units (units 5 to 10). The fault with a minimum accumulated
169 displacement of 2.5m separating both blocks affects the lower levels identified of the fan
170 (5 to 7) and is sealed by the uppermost ones (9-10).

171

172 *La Piedra Menuda trench site*

173 An antithetic scarp to the Cofradía fault was investigated at two 15 and 17 m long
174 trenches perpendicular to the fault with the aim of detecting ruptures affecting the
175 historical Masaya lava flows (280 and 178 yr BP, **Fig. 1c, supplementary Figure S3**).
176 These flows are presumably covered in that site by a very recent small alluvial fan, which
177 onlaps a scarp developed on older Holocene deposits. Neither the main fault nor the lava
178 flow was reached by trenching. Only the southernmost of the two trenches showed faults
179 affecting a volcanic deposits and a related colluvial deposit (**Fig. 2c**). We could not date
180 the colluvial deposits, although they appear to be relatively recent according to its low

181 degree of pedogenesis. The volcanic deposit forms a scarp affected by toppling and is
182 made up of a sequence of volcanic tuff attributed to the Masaya group, probably deposited
183 during the Holocene (**Fig. 2c**). The other trench showed the very recent alluvial fan
184 apparently overlying the fault and containing plastic bottles, baby clothes, plastic bags,
185 etc. It lies on an undisrupted clastic unit that yielded a piece of charcoal dated 1333±45
186 yr BP. This age is older than the missing in the trench site lava flows, probably owing to
187 its irregular contour. So, this fault strand seems to have been quiet since 1333±45 yr BP.

188

189 **Paleoseismological evidences** The interpretation of the results obtained from the El
190 Cocal and La Vaquería trenches evidences recent seismic activity of the Cofradía fault.
191 The Piedra Menuda trenches are not considering in this section due to high rate of
192 sedimentation that avoid reaching paleoseismic evidences by trenching.

193 *El Cocal area*

194 In El Cocal trench, among twenty two samples were taken but only five of them yielded ¹⁴C
195 dating results. Three samples consisted of characteristic pottery fragments, which
196 allowed constraining the ages of the different units (**Table 1, Fig. 2a**). Accordingly, the
197 first stratigraphic sequence (units *w* to *y*) is Middle Holocene in age, whereas the second
198 sequence (units *e* to *a*) consists of historical sediments.

199

200 Evidence of the oldest seismic activity is reflected by liquefaction structures (**Fig.**
201 **2a**, columns 0 -7, northern and southern walls) in beds belonging to Group 1 (units *w* and
202 *x*). Since no liquefaction is observed in Group 2, we suspect that this seismic activity
203 should have occurred in the middle of the Holocene, although no individual events can
204 be determined with the available data.

205 In relation to the deposits of the Group 2, four paleoseismic events were deduced,
206 three of them relatively well constrained on time. From younger to older these events are
207 (**Fig. 2a** and **Fig. 3**):

208 - **Event 4.** Fault F2 displaces the base of unit *a* by a maximum of 0.3 m. The fault vanishes
209 progressively upwards inside the massive unit *a*. The topographical surface does not show
210 any scarp at the prolongation of this fault. However, we consider that this displacement
211 could have affected the upper part of this unit. Reworking of the upper part of unit *a*
212 during strong storms cannot be discarded, as it occurred during the floods related to
213 Hurricane Mitch in 1998. In addition, the upper part of unit *a* is strongly bioturbated. This
214 could explain the upwards vanishing of the fault. This event occurred between 1281 calyr
215 BP and short before present.

216 - **Event 3.** Fault F1 cuts the base of unit *e*, but does not displace the base of unit *a*, which
217 lies on an erosional surface. During event 3 the vertical displacement on fault F2 after
218 restoration of event 4 is 0.3 m. A minimum of 0.30 m is observed on fault F1 (the
219 base of *e* does not crop out in the downthrown wall). Since unit *e* was completely eroded
220 east of F2 before deposition of *a*, the contribution of faults located east of F2 to the total
221 displacement of this event is unknown. The minimum vertical displacement for this event
222 is 0.6 m. Notice that the absence of units *d* and *c* east of columns 19-20 does not allow us
223 to observe the relationship of faults F1 and F2 with these units. Event 3 occurred after
224 deposition of *e* and before the deposition of *a*, i.e., in the time span between 1650 and 600
225 yr BP).

226 - **Event 2.** The wedge shaped breccia, unit *e*, is interpreted as a colluvial wedge resulting
227 from activity on fault F2. Prior to deposition of unit *a*, unit *e* was totally eroded east of
228 F2. The maximum observable thickness of unit *e* is 0.8 m (southern wall, west of F1).
229 Taking into account that part of this unit was eroded, its original thickness was surely

230 larger. As a consequence the displacement along the fault responsible for event 2 was
231 likely greater than 1 m. F2 is more likely to have caused the colluvial wedge and not the
232 faults located to the east (F3 and F4). These faults have too small associated
233 displacements as to generate such a thick wedge (e). This event occurred shortly before the
234 deposition of unit e, constrained by 1650 yr BP (maximum age of e) and 1150 calyr BP
235 (minimum age of e assuming it is older to unit c, which is dated as 1411 ± 109 calyr BP).

236 **-Event 1.** Several features evidence an older event: 1) Faults displacing the base of unit
237 x, but not affecting the base of e, which lies on an erosional surface. 2) The different
238 thicknesses (or presence/absence) of unit x on both sides of the fault zone suggest
239 differential erosion related to uplift on the eastern wall following deposition of x. This
240 erosion hid out the behavior of faults east on F2 during this event. This event is
241 constrained by maximum age of unit w (7831 calyr BP) and the minimum age of unit e
242 (given by age of unit c, 1150 calyr BP).

243

244 *La Vaquería area*

245 Units 5 and 7 were interpreted as colluvial wedges owing to their lithology and
246 geometry. This data suggests at least a minimum of two seismic events prior to the
247 deposition of unit 9: event 3 is evidenced by the fault cutting colluvial wedge 7, and event
248 2, by the deposition of this colluvial wedge. The flexure of Unit 9 (south wall) could be
249 relate with the latest event. An older event (event 1) is probable, if the interpretation of
250 unit 5 as a colluvial wedge is correct. Unfortunately, only a piece of charcoal taken from
251 the lower part of unit 5 was available for dating at this site (7062 ± 254 calyr BP),
252 suggesting an approximate age for the oldest event. The two younger events postdate it,
253 but their age could not be constrained, although the flexure of unit 9.

254

255

256 **Discussion**

257 We focussed the discussion on the data corresponding to the last three events
258 observed in El Cocal trench, which are better constrained in age. At this site the fault zone
259 is located at the lake shore, where sedimentation and erosive processes alternate. In spite
260 of this, the last three events, which occurred in historical times, are relatively well
261 recorded.

262 *Slip rate.* The total minimum vertical displacement observed for the last three
263 events is 1.9 m (event 2: 1 m, event 3: 0.28 + 0.30 m; event 4: 0.32 m). So, for the last
264 1714 - 1398 yr BP, i.e., since the occurrence of the second event, the minimum vertical
265 slip is 1.1 – 1.3mm/year. This is a minimum value since displacements along faults east
266 of fault F2, tilting of beds, and the eroded part of unit *e* were not considered. Therefore,
267 this short term vertical slip rate value matches well with the 1.2 mm/year mid-term slip
268 rate suggested by Cowan et al. (2000) for the area, and is larger than the 0.3-0.9 mm/a
269 slip rate estimated by Cowan et al. (2002) for the seismogenic Aeropuerto fault.

270 To corroborate the four deduced paleoseismic events along the geological section
271 in El Cocal trench, a vertical slip rate of 1.1 mm/year was considered, based on observed
272 deformation, to perform a retrodeformation analysis, using layer *x* as a reference marker
273 in the surface flexure (**Fig. 4**). This flexure seems controlled by the splay of faults
274 developed at the upwards termination of the Cofradía fault. We did not take into account
275 faults east of F2 in the restoration since, to draw a plausible section, their offsets need to
276 be small and thus, negligible. Moreover, the amount of these offsets is unknown because
277 of erosion prior to deposition of unit *a*. Restoration of events 2 to 4 along faults F1 and F2
278 shows a total recovery of F1 and an important recovery of F2. A total recovery of F2
279 could be probably obtained if the total thickness of the wedge *e* were taken into account

280 instead of only the preserved part. The possible tilting of the beds during these events was
281 not considered. The remaining offset of bed *x* west of F1 has to be attributed to the activity
282 of faults located west of F1 and to events occurring between ca. 7000 and 1650– 1150 cal
283 yr BP.

284 We calculated the maximum magnitude expected from our results. The minimum
285 vertical displacement of the surface for the maximum event observed is ca 1 m (event
286 2). This value correspond to a minimum magnitude of $M_w = 6.78$, and a minimum fault
287 length of 24 km according to empirical relationships for normal faults (Wells and
288 Coopersmith, 1994). Such a length is under the total length mapped for the Cofradia fault
289 trace (39 km). Since the observed displacements are minimum values in this site, and
290 other scarps eastwards have been described across the same section (Dames and Moore-
291 Lamsa, 1978), it is reasonable to accept that the entire Cofradia fault is capable of rupture
292 in a single event. Updated relationships proposed by Villamor et al. (2001) are
293 recommended by Stirling et al. (2013) for normal faults in volcanic environments with
294 crustal thickness greater than 10 km, as is the case of the Nicaraguan depression (e.g.,
295 Cáceres, 2003; Mackenzie et al., 2008), suggest a maximum M_w of 7 ($\sigma = 0.34$) for a 39
296 km long surface fault trace.

297

298 *Recurrence.* The last three events (E2, E3, E4) have occurred since the time of
299 event 2 (E2), i.e., since 1650 yr BP as the older and 1150 cal yr BP as the younger possible
300 date. If we considered that the 1865 earthquake was generated by the Cofradia fault and
301 it is our event 4 at el Cocal, a time span of 1249 – 1565 yr will cover the three events,
302 corresponding to two seismic cycles of minimum 624.5 yr and maximum 782.5
303 yr. Assuming the last event was that of 1865, any of these seismic cycle boundaries

304 matches with the event chronology obtained here for the last 3 events (**Fig. 3**), which
305 point out that the fault could have a characteristic behavior.

306

307 *Last event.* Only the oldest possible age of the last event was constrained. This event
308 (event 4 at El Cocal) occurred between 1281 calyr BP and short Before Present. The
309 catalog of Nicaraguan earthquakes compiled by Leeds (1974) begins on 1520 (sixteen
310 century) and that of Central America done by Peraldo and Montero (1999) on 1530.
311 Leeds' catalog includes a larger number of earthquakes than Peraldo and Montero's
312 catalog, but this latter one offers more detailed information on some particular
313 earthquakes. Leeds classifies the earthquakes in five classes, from A (the largest
314 earthquakes) to E (the smallest ones), and assigns an arbitrary body-wave magnitude to
315 all events for which no magnitude has been previously published. The largest earthquakes
316 affecting western Nicaragua are B-class earthquakes: three during XVII century (1609,
317 1648 and 1663), the earthquake of May 1844 and that of February 1866 (Leeds, 1974). It
318 is likely that the last event described here could correspond to one of the aforementioned
319 earthquakes. The descriptions of surface alterations along the Tipitapa River during the
320 earthquakes of 1865-1866 described in Montessus de Ballore (1888) lead us to propose
321 the Cofradia fault as the most probable source of this earthquake. The time range for event
322 4 at the El Cocal site is compatible with that date. Additionally, the Cofradia fault is the
323 closest fault to the Tipitapa River (**Fig. 1b and c**) with known geomorphic expression.

324

325 **Conclusion**

326 The paleoseismological data compiled in this work provide new insight into the
327 seismogenic behavior and earthquake history of the Cofradia fault. The maximum rupture
328 length is 39 km and its minimum vertical slip rate is 1.1 – 1.3 mm/year. The maximum

329 earthquake magnitude of the fault is likely to be around 6.9 ± 0.1 , with a mean recurrence
330 interval between 624.5 and 782.5 yr.

331 Among the three paleoseismic sites studied, El Cocal (central part of the trace)
332 supplied the most complete record of seismic events. At both La Vaquería (north-central
333 part of the trace) and El Cocal site, middle Holocene events were identified, one of them
334 probably occurring before 7062 ± 254 cal yr BP. The younger events recorded at El Cocal
335 are named event 2, occurring between 1650 yr BP and 1150 cal yr BP; event 3, taking place
336 between 1650 and 600 yr BP; and event 4, which probably took place a short time before
337 the present and after 1281 cal yr BP. Any of those events could match with the two
338 younger events recorded at La Vaquería, which suggest common surface ruptures of these
339 parts of the fault.

340 Accordingly, the Cofradia fault is a probable source of the Nicaraguan earthquakes (1865
341 – 66, $M = 7-7.7$, [Peraldo and Montero \(1999\)](#)), which may coincide with the last
342 paleoseismic event (E4). This is the most conspicuous fault with geomorphological
343 expression crossed by the Tipitapa River, which suffered surface alterations during those
344 historical events. Moreover, the surface trace of the Cofradia fault (39 km), in case of a
345 complete rupture, can have a maximum moment magnitude $M_w = 7$, which is consistent
346 with the 1865-66 events estimated earthquake magnitudes.

347

348 **Data and Resources**

349 All data used in this paper come from published sources listed in the references.

350

351 **Acknowledgments**

352 The RISK NAT group is partly founded by the 2009-SGR-520 AGUR project. Stays of
353 C. Rubí in Barcelona to prepare his PhD thesis were funded by ASDI-Sweden in the

354 frame of the Proyecto Multidisciplinario de Investigación Ambiental (PMIA), Nicaragua.
355 Trenching campaign was conducted during the dry season of 2007 with the help of Oriol
356 Piqué and the financial support of Spanish projects CGL 2006-27 072 E/BTE and AECI
357 C/6111/06.

358

359

360 **References**

- 361 Alvarado, D., C. DeMets, B. Tikoff, D. Hernández, T. F. Wawrzyniec, C. Pullinger, G. Mattioli,
362 H. L. Turner, M. Rodríguez and F. Correa-Mora (2011). Forearc motion and
363 deformation between El Salvador and Nicaragua: GPS, seismic, structural, and
364 paleomagnetic observations. *Lithosphere* **3(1)** 3-21.
- 365 Brown, Jr., R.D., P.L. Ward and G. Plafker (1973). Geologic and seismologic aspects of the
366 Managua, Nicaragua, earthquakes of December 23, 1972, *Geol. Surv. Prof. Pap.* **838**
367 34pp.
- 368 Cáceres, D. (2003). Earthquake Sources and Hazard in Northern Central America.
369 Comprehensive Summaries of Uppsala Dissertations, Uppsala University, 28 pp.
- 370 Cowan, H., M. N. Machette, X. Amador, K. S. Morgan, R. L. Dart and L. A. Bradley (2000).
371 *Map and Database of Quaternary Faults in the Vicinity of Managua, Nicaragua*. Open-
372 File Report , 00-437.
- 373 Cowan, H., D. Pantosti, P. Martini, W. Strauch, and Workshop Participants (2002). Late
374 Holocene Earthquakes on the Aeropuerto Fault, Managua, Nicaragua, *Bull. Seism. Soc.*
375 *Am.* **92** 1694-1707.
- 376 Dames and Moore-Lamsa (1978). *Informe final del Estudio geológico de las ciudades del*
377 *sistema metropolitano: Managua, Nicaragua*, Vice Ministerio de Planificación Urbana,
378 Managua, 143 pp.

379 DeMets, C., R.G. Gordon, D.F. Argus, and S. Stein (1994). Effect of recent revisions to the
380 geomagnetic reversal time scale on estimate of current plate motions, *Geophys. Res.*
381 *Lett.* **21** 2191-2194.

382 Dewey, J.W. and T. Algermissen (1974). Seismicity of the Middle America Arc-trench System
383 near Managua, Nicaragua. *Bull. Seism. Soc. Am.* **64(4)** 1033-1048.

384 Durham, H.W. (1931). Managua – Its Construction and Utilities. *Engineering News-Record* 696-
385 700.

386 Ferrez Weinberg, R. (1992). Neotectonic development of western Nicaragua. *Tectonics* **11(5)**
387 1010-1017.

388 Frischbutter, A. (2002): Structure of the Managua graben, Nicaragua, from remote sensing
389 images. *Geofisical Internacional* **41(2)** 87-102.

390 Funk, J., P. Mann, K. McIntosh, and J. Stephens (2009). Cenozoic tectonics of the Nicaraguan
391 depression, Nicaragua, and Median trough, El Salvador, based on seismic-reflection
392 profiling and remote sensing data, *Bull. Geol. Soc. Am.* **121(11-12)** 1491-1521.

393 García Vásquez, R. (1996). Hallazgos recientes en Acahualinca (N-Ma-61), in *La segunda*
394 *temporada del proyecto “Arqueología de la Zona Metropolitana de Managua”*
395 Frederick W. Lange, (Editor, Managua, 99-102.

396 Girard, G. and B. Van Wyk de Vries (2005). The Managua Graben and Las Sierras-Masaya
397 volcánico complex (Nicaragua); pull-apart localization by an intrusive complex: results
398 from analogue modelin. *J. Volcanology and Geothermal Res.* **144** 37-57.

399 Grases, J. (1974). *Sismicidad de la Región Centroamericana asociada a la Cadena volcánica*
400 *del Cuaternario*. 2. Instituto de Geociencias, Caracas, 253 pp.

401 La Femina, P., T. H. Dixon, and W. Strauch (2002). Bookshelf faulting in Nicaragua. *Geology*
402 **30(8)** 751-754.

403 Leeds, D. J. (1974). Catalog of Nicaraguan earthquakes, *Bull. Seis. Soc. Am.* **64** 1135-1158.

404 MacKenzie, L., G. A. Abers, K. M. Fischer, E. M. Syracuse, J. M. Protti, V. Gonzalez, and W.
405 Strauch (2008), Crustal structure along the southern Central American volcanic front,
406 *Geochem. Geophys. Geosyst.*, **9**, Q08S09, doi:10.1029/2008GC001991.

407 Martínez, W., and E. Noguera (1992). Geological framework of earthquakes occurrence in
408 Nicaragua, Central America, *J. Geol. Soc. Japan* **98** 165-176.

409 Montessus de Ballore, F. (1888). *Tremblements de terre et éruptions volcaniques en Centre*
410 *Amérique depuis la conquête espagnole jusqu'à nos jours*. Soc. Sci. Nat de Saone et
411 Loire., Dijon, 233 pp.

412 Peraldo, G., and W. Montero (1999). *Sismología histórica de América Central*, IPGH, México,
413 347 pp.

414 Reimer, P. J., E. Bard, A. Bayliss, J. W. Beck, P. G. Blackwell, C. Bronk Ramsey, C. E. Buck, H.
415 Cheng, R. L. Edwards, M. Friedrich, P. M. Grootes, T. P., Guilderson, H. Haflidason, I.
416 Hajdas, C. Hatté, T. J. Heaton, D. L. Hoffmann, A. G. Hogg, K. A. Hughen, K. F.
417 Kaiser, B. Kromer, S. W. Manning, M. Niu, R. W. Reimer, D. A. Richards, E. M. Scott,
418 J. R., Southon, R. A. Staff, C. S. M. Turney and J. van der Plicht (2013). IntCal13 and
419 Marine13 radiocarbon age calibration curves 0-50,000 years cal BP. *Radiocarbon*, **55**(4),
420 1869-1887

421 Ruano, P, C. Rubí, E. Masana, M. Ortuño, O. Piqué, and P. Santanach (2008). Paleosismología
422 en la falla de Cofradía, Managua, Nicaragua: resultados preliminares, *Geo-Temas* **10**
423 1059-1062.

424 Stirling, M., T. Goned, K. Berryman, and N. Litchfield (2013). Selection of Earthquake Scaling
425 Relationships for Seismic-Hazard Analysis. *Bull. Seism. Soc. Am.* **103**(6) 1–19, doi:
426 10.1785/0120130052.

427 Stuiver, M. and P. J. Reimer (1993). *CALIB User's Guide Rev. 3.0*. University of Washington,
428 Quaternary Isotopes Laboratory.

429 Sultan, D. I. (1931). The Managua earthquake, *Military Engr.* **23** 354-361.

430 Villamor, P., R. K. R. Berryman, T. Webb, M. Stirling, P. McGinty, G. Downes, J. Harris,
431 and N. Litchfield (2001). *Waikato Seismic Loads: Revision of Seismic Source*
432 *Characterisation*, GNS Client Report 2001/59.

433 Ward, P, J, Gibbs, D. Harlow, and Q. Aburto (1974). Aftershocks of the Managua, Nicaragua,
434 Earthquake and the Tectonic Significance of the Tiscapa Fault, Bull.Seism. Soc. Am.
435 **64(4)** 1017-1029.

436 Wells, D.L., and K.J.Coppersmith (1994): New empirical relationships among magnitude,
437 rupture length, rupture width, rupture area, and surface displacement, Bull. Seism. Soc.
438 Am. **84(4)** 974-1002.

439

440 **Figures and Tables**

441 **Figure 1.** Geodynamical and geological setting. a) Middle America Volcanic Chain in
442 plate tectonic framework. b) Managua graben in the Nicaraguan Depression. Location in
443 Fig 1a. AF, Airport Fault; CF, Cofradía Fault; EF, Estadio Fault; MF, Mateare
444 Fault; NMF, Nejapa-Maraflones alignment; TF, Tiscapa Fault. c) Deeper eastern Managua
445 graben area showing the southern sector of Cofradía Fault and trench locations.

446 **Figure 2.** Logs of the El Cocal (a) and La Vaqueria (b) trenches showing the location of
447 main faults and dating samples. A photolog of Piedra Menuda trench (c) is included. The
448 main fault is suggested by the white arrows.

449 **Figure 3.** Paleoearthquake chronology of the studied sites. In the upper part of the graph,
450 the dating results for the el Cocal trench are plotted. In the lower part, the event time
451 constraints for the El Cocal and La Vaqueria are determined by the age of the
452 corresponding bracketing units.

453 **Figure 4.** Retrodeformation scheme for the El Cocal trench North wall. a) Schematic
454 cross section of Present day geometry after event 4, including a reconstruction of the
455 eroded and buried continuation of marker layer *x*. The depth of layer *x* in the down-thrown
456 wall was calculated by considering an approximate age of 5,000 BP for it and a 1.1
457 mm/year vertical slip rate for the Cofradia fault. b) Geometry of layers after event 3. c)
458 Geometry of layers after event 2, showing a total recovery of fault 1. d) Geometry of layers

459 previous to event 2 still shows a slight flexure of x, probably associated to faulting along
460 other secondary faults of the splay and along the main faults at depth.

461 **Table 1.** Dating results for the samples taken at El Cocal, La Vaqueria and La
462 PiedraMenuda trenches.

463 **Online Supplementary Material**

464 **Figure S1.** Photomosaic of the El Cocal trench, N and S walls.

465 **Figure S2.** Photomosaic of the La Vaqueria trench, N and S walls.

466 **Figure S3.** Photomosaic of the PiedraMenuda trench, S wall.

467

Table 1. Dating results

Trench (Unit)	Sample	14C age* (yrs BP)	Calibrated age ** or archeological age (yrs)	Material/consideration
El Cocal (<i>w</i>)	MCN-3	6890±40	5794 ± 87 BC	Mollusc
El Cocal (<i>w</i>)	MCN-13	5960±30	4853 ± 84 BC	Charcoal
El Cocal (<i>e</i>)	MCS-7		300-800 AD	Pottery fragment-trichromed Tola type, attributed to Bagaces cultural period
El Cocal (<i>c</i>)	MCS-6	1490±40	579 ± 37 AD	Charcoal/ preferred age for the unit
El Cocal (<i>c</i>)	MCN-1		300-800 AD	Pottery fragment attributed to Bagaces cultural period
El Cocal (<i>a</i>)	MCS-5	2020±30	24 BC ±82	Charcoal, reworked fragments
El Cocal (<i>a</i>)	MCN-5		800-1350 AD	Pottery fragment-striated Sacasa type attributed to Sapoá cultural period
El Cocal (<i>a</i>)	MCN-11	1260±30	726 AD ±57	Charcoal
El Cocal (<i>a</i>)	MCN-9		800-1350 AD	Pottery fragment-Papagayo type attributed to Sapoá cultural period
La Vaqueria-2 (5)	MVS2-1	6200±95	5136 ± 230 BC	Charcoal
Piedra Menuda	MPN2-4	1420±35	630 ± 22 AD	Charcoal

* Conventional radiocarbon ages reported by NOSAMS. Calculations assume a Libby half-life (5568 yr). Uncertainties are 1 Standard deviation counting errors.

** Dendrochronologically calibrated, calendar age ranges from CALIB 5.1 software (Stuiver and Reimer, 1993), 2 standard deviation uncertainty and the INTCAL04.14c curves (Reimer et al. 2004)

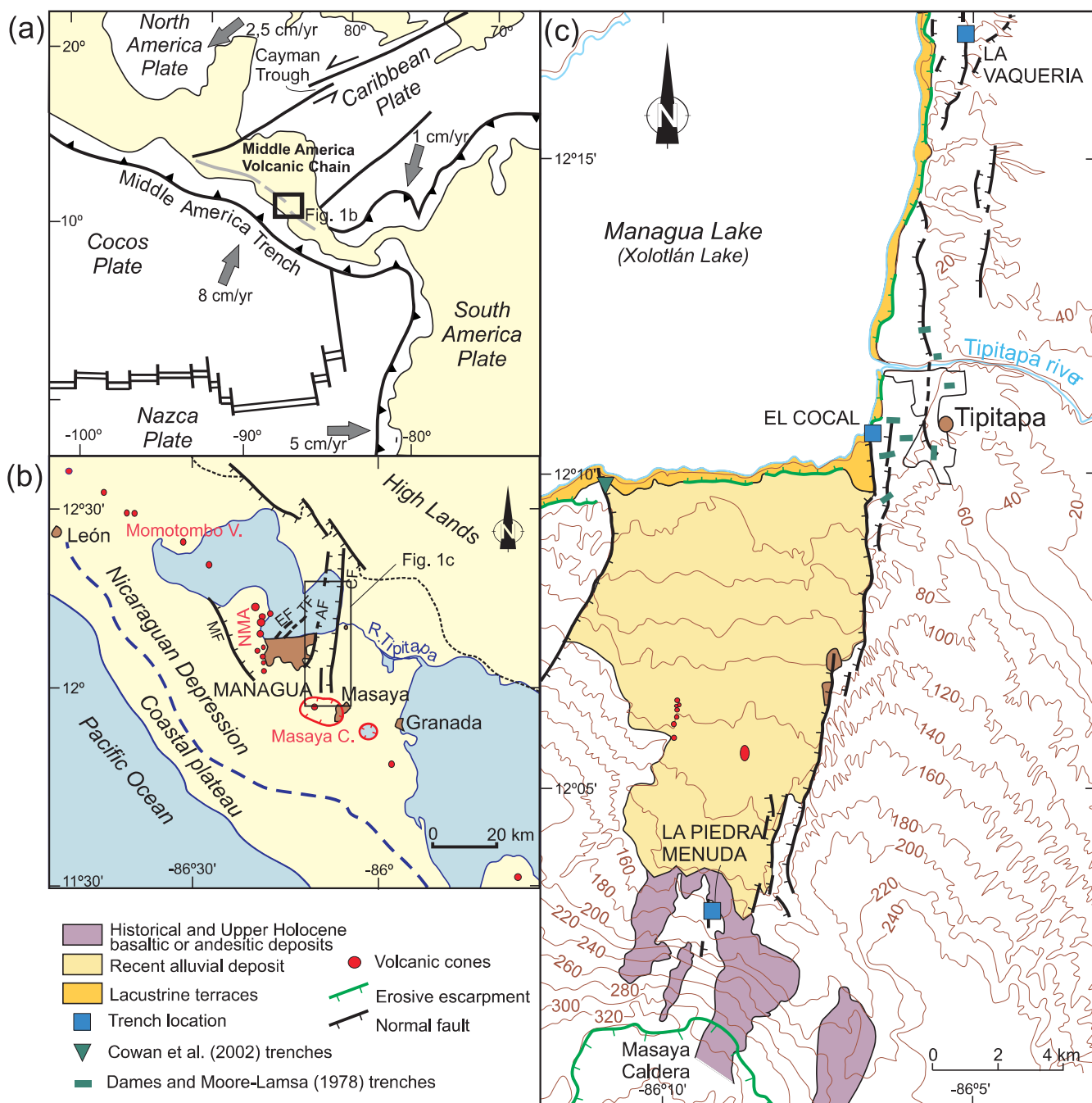


Fig. 1 Geodynamical and geological setting. a) Middle America Volcanic Chain in plate tectonic framework. b) Managua graben in the Nicaraguan Depression. Location in Fig 1a. AF, Airport Fault; CF, Cofradía Fault; EF, Estadio Fault; MF, Mateare Fault; NMF, Nejapa-Maraflor alignment; TF, Tiscapa Fault. c) Deeper eastern Managua graben area showing the southern sector of Cofradía Fault and trench locations.

Figure 2
[Click here to download Figure: Fig. 2 new.pdf](#)

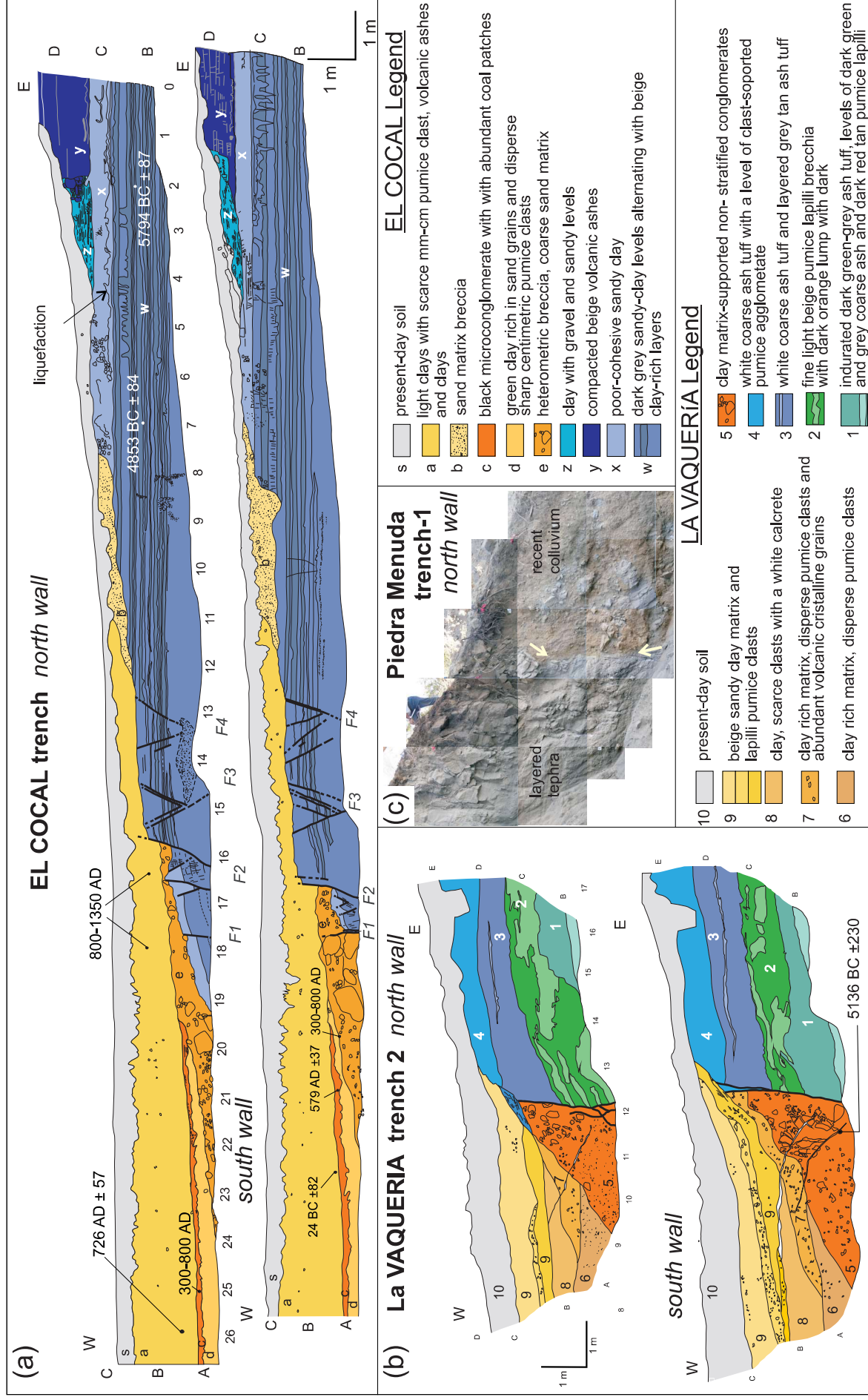


Figure 2. Logs of the El Cocal (a) and La Vaqueria (b) trenches showing the location of main faults and dating samples. A photolog of Piedra Menuda trench (c) is included. The main fault in Piedra Menuda is suggested by the arrows on top of the photograph.

Figure 3

[Click here to download Figure: Fig. 3 new.pdf](#)

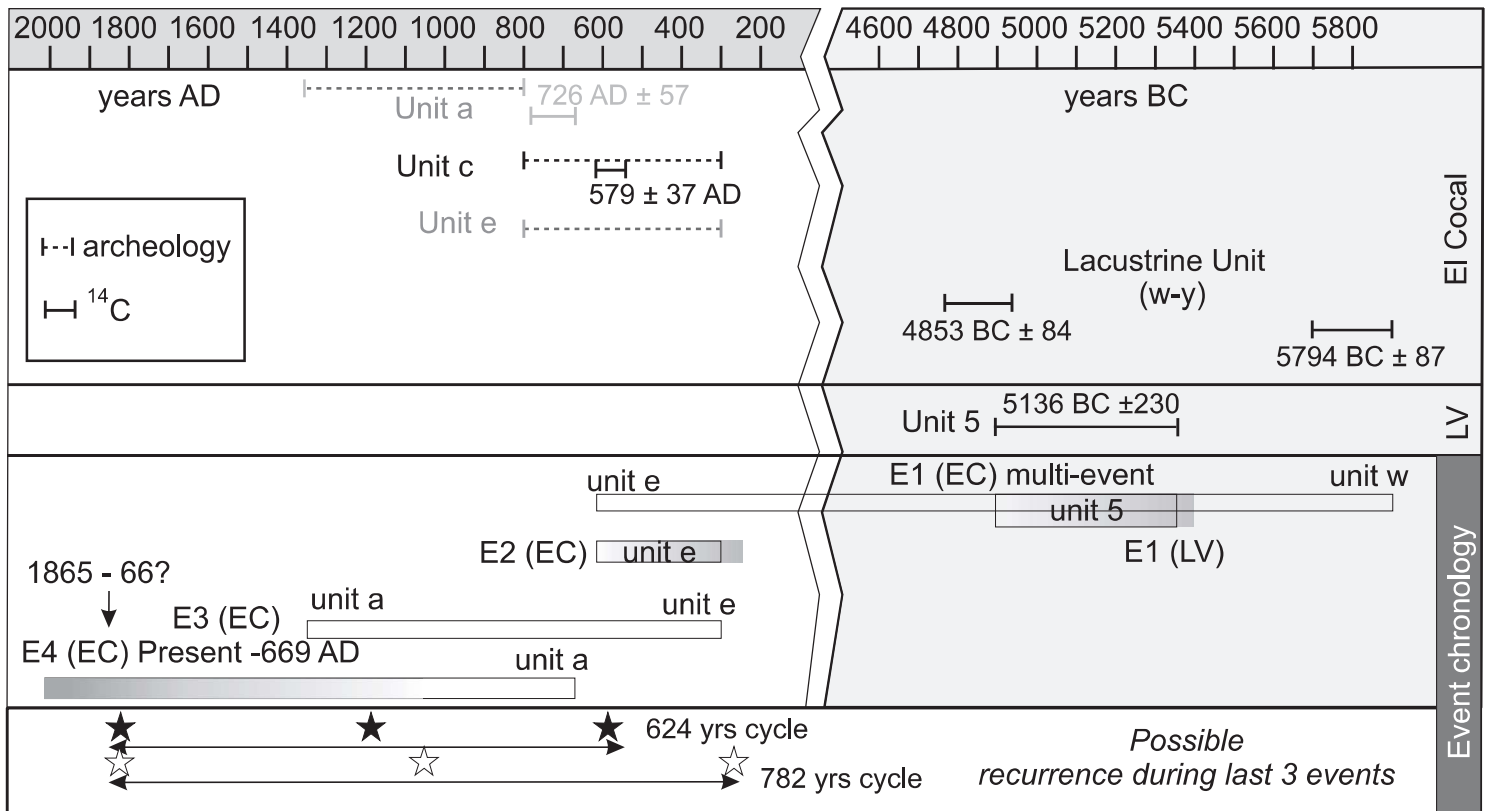


Figure 3. Paleoseismicity chronology of the studied sites. In the upper part of the graph, the dating results for the el Cocal trench are plotted. In the lower part, the event time constraints for the El Cocal and La Vaqueria are determined by the age of the corresponding bracketing units.

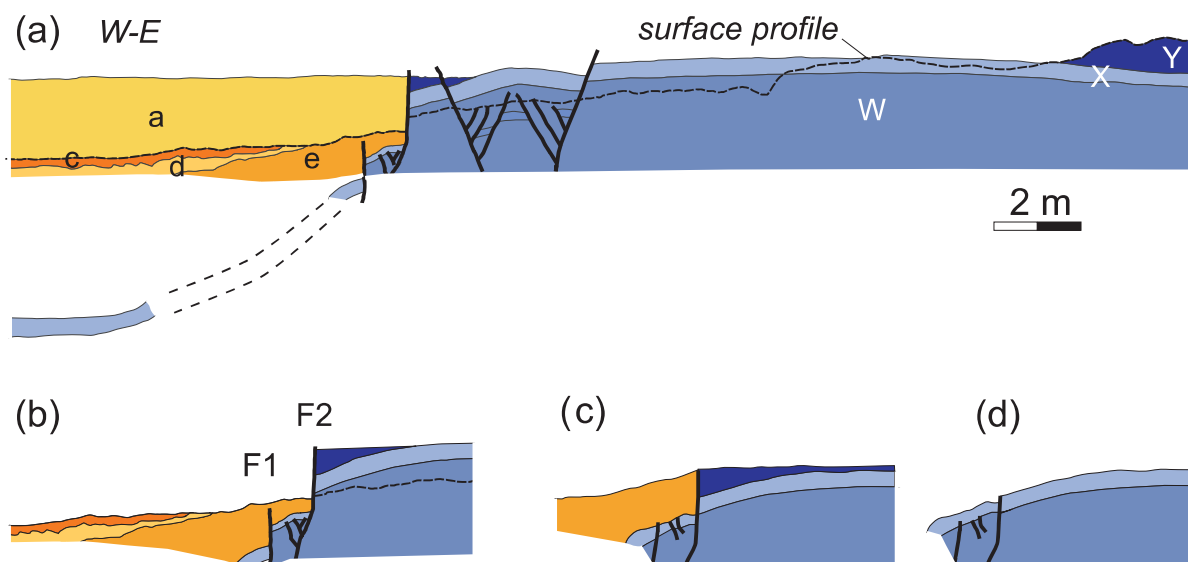


Figure 4. Retrodeformation scheme for the El Cocal trench North wall. a) Schematic cross section of Present day geometry after event 4, including a reconstruction of the eroded and buried continuation of marker layer x. The depth of layer x in the down-thrown wall was calculated by considering an approximate age of 5,000 BP for it and a 1.1 mm/year vertical slip rate for the Cofradia fault. b) Geometry of layers after event 3. c) Geometry of layers after event 2, showing a total recovery of fault 1. d) Geometry of layers previous to event 2 still shows a slight flexure of x, probably associated to faulting along other secondary faults of the splay and along the main faults at depth.

Electronic Supplement

Manuscript title: On the search for the source of the 1865-66 Nicaraguan earthquakes: paleoseismic data from the Cofradía fault, Managua graben (Nicaragua)

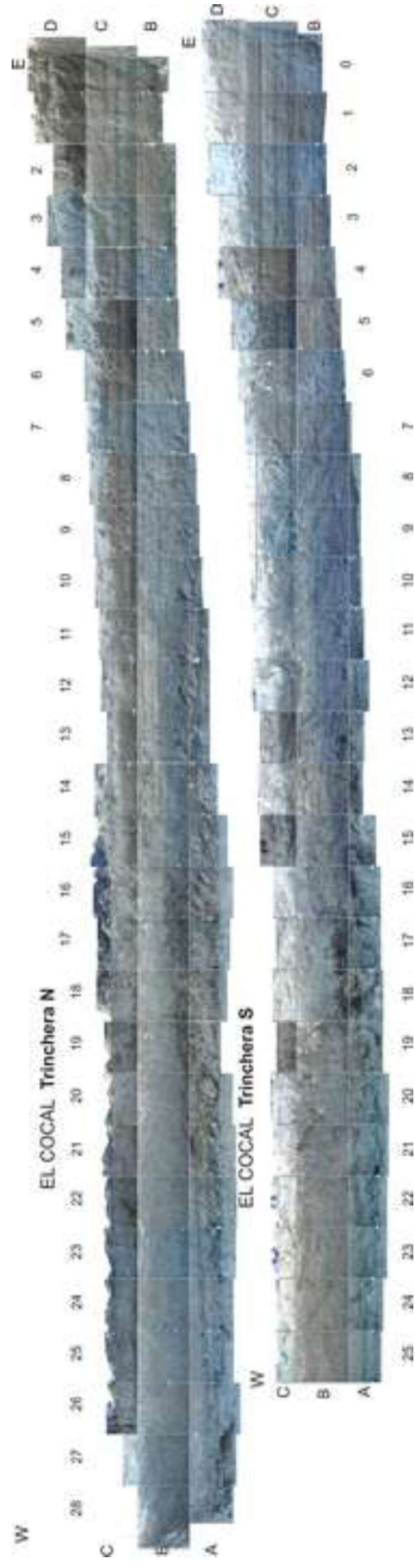
Authors: P. Santanach, P. Ruano, M. Ortuño, C. Rubí and E. Masana

This electronic supplement contains high resolution photomosaics of the walls of the studied trenches.

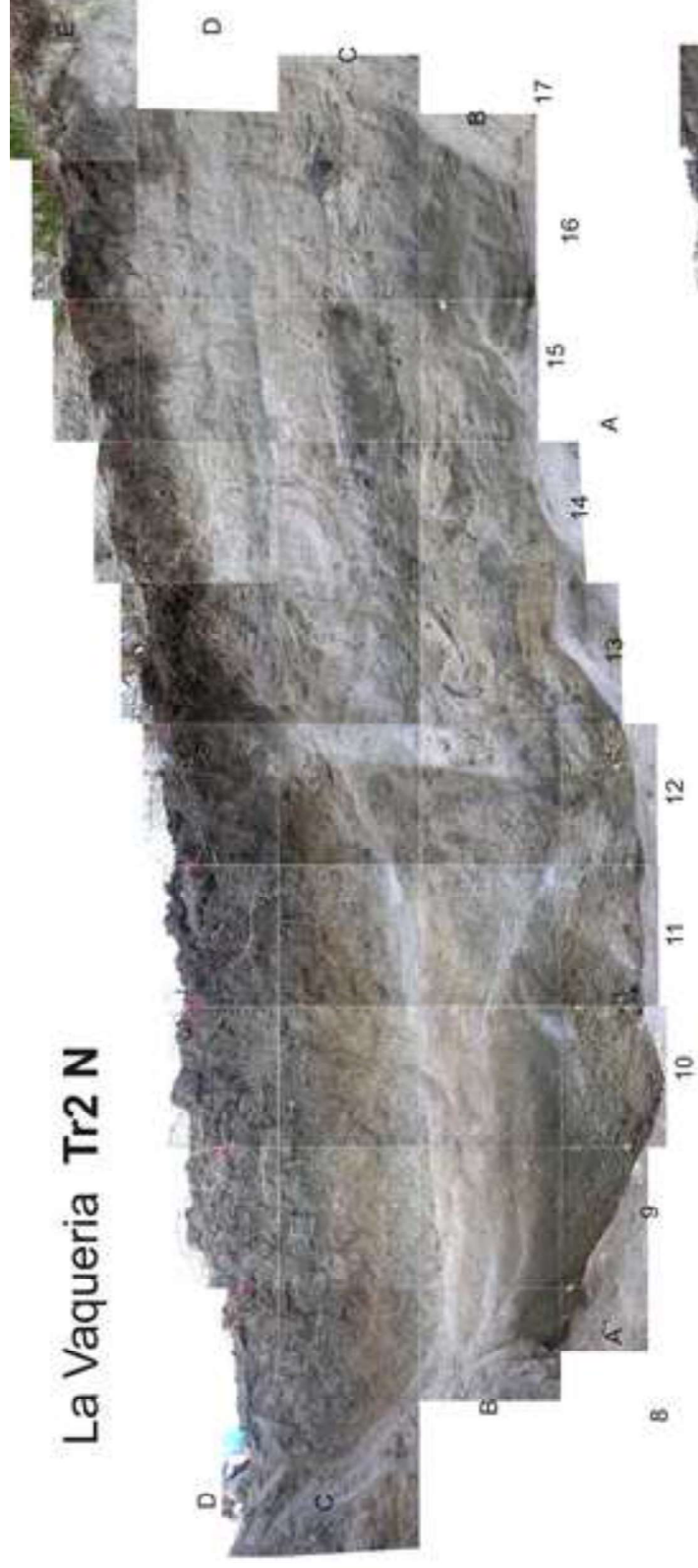
Figure S1. Photomosaic of the El Cocal trench, N and S walls.

Figure S2. Photomosaic of the La Vaqueria trench, N and S walls.

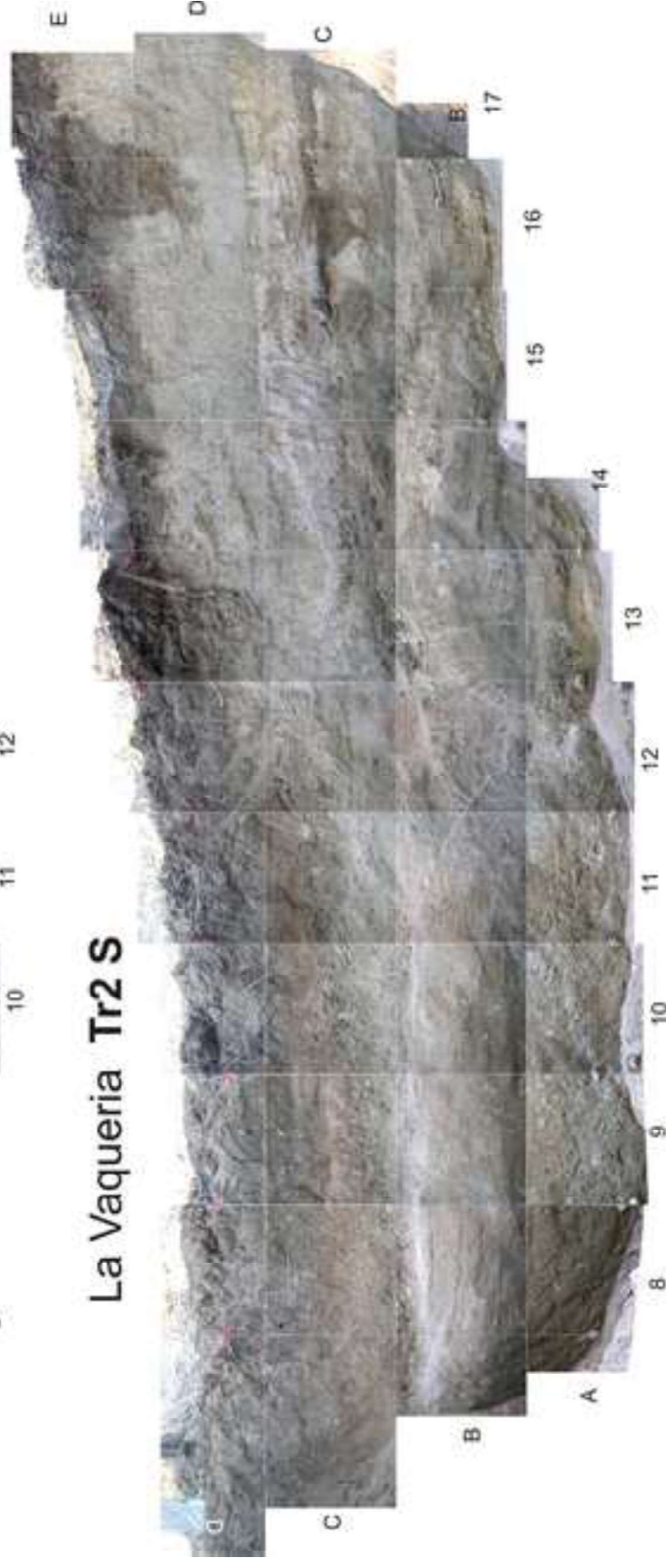
Figure S3. Photomosaic of the **El Cocal** trench, S wall.



La Vaqueria Tr2 N



La Vaqueria Tr2 S



photomosaic Piedra Menuda
[Click here to download high resolution image](#)

